DDR1 triggers epithelial cell differentiation by promoting cell adhesion through stabilization of E-cadherin

Yi-Chun Yeh[a], Chia-Ching Wu[b], Yang-Kao Wang[c], and Ming-Jer Tang[a,d,e]
[a]Institute of Basic Medical Sciences, [b]Department of Cell Biology and Anatomy, [c]Department of Medicine, Skeleton-Joint Research Center, [d]Department of Physiology, and [e]Center for Gene Regulation and Signal Transduction, National Cheng Kung University Medical College, Tainan, Taiwan

ABSTRACT **Discoidin domain receptor 1 (DDR1) promotes E-cadherin–mediated adhesion. The underlying mechanism and its significance, however, have not been elucidated. Here we show that DDR1 overexpression augmented, whereas dominant negative mutant (DN-DDR1) or knockdown of DDR1 inhibited E-cadherin localized in cell-cell junctions in epithelial cells. DDR1 changed the localization and abundance of E-cadherin, as well as epithelial plasticity, as manifested by enhancement of microvilli formation and alteration of cytoskeletal organization. DDR1 also reduced protein abundance of mesenchymal markers, whereas DN-DDR1 and sh-DDR1 showed opposite effects. These results suggest that expression of DDR1 increases epithelial plasticity. Expression of DDR1 augmented E-cadherin protein levels by decreasing its degradation rate. Photobleaching and photoconversion of E-cadherin conjugated with Eos fluorescence protein demonstrated that DDR1 increased the stability of E-cadherin on the cell membrane, whereas sh-DDR1 decreased it. Pull-down assay and expression of constitutively active or dominant-negative Cdc42 showed that DDR1 stabilized E-cadherin through inactivation of Cdc42. Altogether, our results show that DDR1 promotes cell-cell adhesion and differentiation through stabilization of E-cadherin, which is mediated by Cdc42 inactivation.**

Monitoring Editor
Alpha Yap
University of Queensland

Received: Aug 6, 2010
Revised: Jan 10, 2011
Accepted: Jan 26, 2011

INTRODUCTION

Discoidin domain receptor (DDR) was first identified in the slime mold *Dictyostelium discoideum* as Discoidin I (van der Geer *et al.*, 1994), and was shown to function in cell adhesion and migration (Springer *et al.*, 1984). DDR1 and DDR2 are two distinct DDR family members which are receptor tyrosine kinases (RTKs) for collagen (Shelling *et al.*, 1995; Vogel *et al.*, 1997). DDR1 is widely expressed during embryonic development and predominantly expressed in epithelium, particularly in skin, lung, kidney, gut, and brain in adult mice (Zerlin *et al.*, 1993). In contrast, DDR2 is mainly expressed in connective tissue, muscle, heart, and brain (Lai and Lemke, 1991; Vogel, 1999). Although DDR2 shares highly conserved sequences with DDR1, it can only be activated by fibril collagen, particularly types I and III. In contrast, DDR1 is activated by all types of collagen from I to VI. Alternative splicing of DDR1 results in five major isoforms (DDR1a–e) (Perez *et al.*, 1996; Alves *et al.*, 2001). Among the different isoforms, DDR1b is longer than DDR1a by an additional 37 amino acids in the juxtamembrane region, and both are the major types expressed in kidney (Alves *et al.*, 1995).

Functions of DDR1 have been implicated in development given that DDR1 knockout mice are smaller than their littermates and show defects in embryo implantation and mammary gland development. Irregular cell growth and aberrant extracellular matrix deposition in the mammary gland occur in DDR1 knockout mice. During late pregnancy, abnormal differentiation of duct cells is found (Vogel *et al.*, 2001). Using a disease model, Lee *et al.* found that expression of DDR1 does not overlap with staining for α-smooth muscle actin (α-SMA) in the remnant kidney after injury (Lee *et al.*,

This article was published online ahead of print in MBoC in Press (http://www.molbiolcell.org/cgi/doi/10.1091/mbc.E10-08-0678) on February 2, 2011.

Address correspondence to: Ming-Jer Tang (mjtang1@mail.ncku.edu.tw).

Abbreviations used: CHX, cycloheximide; DDR1, discoidin domain receptor 1; DN, dominant negative; EMT, epithelial-to-mesenchymal transition; FLIP, fluorescence loss in photobleaching; HMDS, hexamethyldisilazane; MDCK, Mardin-Darby canine kidney; ROI, region of interest; RT, reverse transcriptase; RTK, receptor tyrosine kinase; SEM, scanning electron microscopy.

2004). Furthermore DDR1-deficient mice demonstrate thick subepithelial glomerular basement membrane with loss of slit diaphragms, which results in proteinuria (Gross *et al.*, 2004). These results highlight the functional role of DDR1 in maintaining cell differentiation. The detailed molecular mechanism, however, is unclear. Our previous studies showed that DDR1 overexpression reduces collagen-induced cell proliferation, extension, and migration, whereas DN-DDR1 enhances these cellular functions (Wang *et al.*, 2005, 2006). In contrast, DDR1 inhibits collagen-induced cell extension by suppressing $\alpha_2\beta_1$ integrin-induced Cdc42 activation (Yeh *et al.*, 2009). These results indicate the opposing functions of DDR1 and $\alpha_2\beta_1$ integrin in the regulation of many cellular events and suggest that the signaling balance between DDR1 and integrins is critical in determining cell fates.

E-cadherin–mediated intercellular adhesion has a central role in maintaining cell polarity and tissue architecture in epithelial cells (Knust and Bossinger, 2002; Nelson, 2003). E-cadherin knockout mice cannot survive after 32-cell trophectoderm stage, which indicates the importance of E-cadherin–mediated cell–cell contact in the early developmental stage (Larue *et al.*, 1994; Ohsugi *et al.*, 1997). The functions of E-cadherin have also been profoundly studied in many pathophysiological conditions. Loss of E-cadherin is generally seen in malignant tumors (Umbas *et al.*, 1994; Cowin *et al.*, 2005; Wheelock *et al.*, 2008) and down-regulation of E-cadherin is taken as a hallmark for the epithelial-to-mesenchymal transition (EMT) (Kalluri and Neilson, 2003). Not only loss of E-cadherin expression but also the inactivation of E-cadherin is sufficient to trigger loss of epithelial plasticity (Zheng *et al.*, 2009), and reexpression of E-cadherin suppresses the malignancy of cancer cells (Vleminckx *et al.*, 1991).

Membrane-bound E-cadherin comprises two main pools, the *trans*-homophilic dimer and the homo-E-cadherin cluster which are displayed by the clustering of *trans*-homophilic dimer of E-cadherin. *Trans*-homophilic E-cadherin exchanges from the monomer pool of E-cadherin on the membrane and exhibits a higher lateral diffusion rate and faster recycling through the endocytic pathway (Leckband and Prakasam, 2006; Pokutta and Weis, 2007). The homo-E-cadherin cluster is relatively stable, and its structure is well-preserved during tissue organization (Cavey *et al.*, 2008). Therefore cell adhesion strength is dependent on homo-E-cadherin cluster (Adams *et al.*, 1998). The *trans*-homo dimer of E-cadherin to neighboring cells recruits downstream β-catenin and p120-catenin. Subsequently β-catenin recruits α-catenin, which links and modulates the organization of the actin cytoskeleton (Tsukita *et al.*, 1992) and forms mature adherent junctions or homo-E-cadherin clusters. As a result, each component in this complex—β-catenin, α-catenin, and actin cytoskeleton—is important in maintaining the stability of adherent junctions (Leckband and Prakasam, 2006).

Many studies have indicated that the activation of RTKs regulates the expression, trafficking, and turnover of E-cadherin (Hoschuetzky *et al.*, 1994; Fujita *et al.*, 2002; Andl and Rustgi, 2005; Kimura *et al.*, 2006). It has also been shown that the interactions of RTKs and E-cadherin attenuate the binding affinity and kinase activity of RTKs (Qian *et al.*, 2004). These results suggest a complex reciprocal regulation between RTK and E-cadherin in regulating adherent junctions. Our recent studies have identified the physical interaction between DDR1 and E-cadherin, which negatively regulates type I collagen-activated DDR1 (Wang *et al.*, 2009). Expression of DDR1, however, can positively regulate E-cadherin–mediated adhesion, but the detail mechanism is still unknown. Therefore we aimed to determine the molecular mechanism underlying the regulation of adherent junctions by DDR1 and its functional relevance.

RESULTS

DDR1 promotes E-cadherin–mediated cell–cell adhesion in normal epithelial cells

To examine the functions of DDR1 in epithelial cell differentiation, we used two clones of LLC-PK1 cells overexpressing myc-tagged DDR1, the DB10, DB21, and one clone of myc-tagged dominant negative DDR1 (DN-DDR1), the DN8 (Figure 1A). After culture for 24 h, control LLC-PK1 cells formed a monolayer of islet-like structure with well-organized cell–cell contacts, typical characteristics of epithelial cells. DB10 cells showed similar characteristics but exhibited more distinct cell boundaries and a more compact phenotype. In contrast, DN8 cells were spindle-shaped and possessed a better spreading ability; these qualities were characterized as the mesenchymal phenotype (Figure 1B). To verify whether these phenotypic changes were elicited by the activation of DDR1, the phosphorylation level of DDR1 was assessed by using phosphospecific antibody, 4G10. In control cells, DDR1 phosphorylation was increased upon collagen stimulation for 24 h. In DB10 and DB21 cells, the phosphorylation of DDR1 was increased without collagen stimulation. On collagen treatment, it induced further phosphorylation of DDR1. In contrast, phosphorylation of DDR1 was suppressed in DN8 cells cultured on collagen-coated dishes (Figure 1C). This result indicates that expression of DDR1 promotes epithelial phenotypic change.

E-cadherin–mediated adherent junctions are critical for the maintenance of epithelial characteristics. To understand the distribution of E-cadherin, we performed an immunofluorescence study to examine the localization of E-cadherin among different DDR1 expression clones. In control cells, less intense E-cadherin staining was found in the cell–cell junctions and colocalized with cortical actin, which was a marker of mature adherent junctions. Other than junctional E-cadherin, punctate staining of E-cadherin was found in the cytosol regardless of collagen treatment. DB10 cells, in both culture dish and collagen-coated dish, displayed strong E-cadherin staining in cell–cell junctions and colocalized with typical cortical actin structure. Less cytosolic E-cadherin was observed in this clone. In contrast, DN8 cells exhibited less junctional E-cadherin but strong punctate staining in the cytosol regardless of collagen treatment. In addition, instead of expressing cortical actin, many stress fibers were formed in DN8 cells (Figure 1D). These results suggest that expression of DDR1 promotes E-cadherin–mediated adhesion and that treatment of collagen is not able to switch DDR1-induced epithelial characteristics.

To understand whether DDR1-triggered localization of E-cadherin in cell–cell junctions was a general phenomenon in epithelial cells, various DDR1 expression clones in NMuMG cells were established. Protein levels of myc-tagged DDR1 (DB11) and DN-DDR1 (DN5) were confirmed (Figure 1E). Immunofluorescence results showed that DB11 cells not only increased E-cadherin staining in cell–cell junctions but also reduced cytosolic E-cadherin staining (Figure 1F). The DN5 cells showed less E-cadherin staining in cell–cell junctions (Figure 1F). To verify the function of endogenous DDR1, we performed specific short hairpin RNA (shRNA) to knock down the expression of DDR1. The shRNA reduced the endogenous DDR1 by ~50% in NMuMG cells (Figure 1G) and by more than 90% in Mardin-Darby canine kidney (MDCK) cells (Figure 1H). Both of the DDR1 knockdown clones showed decreases in E-cadherin staining in cell–cell junctions and increases in cytosolic E-cadherin staining. These results indicate that DDR1-triggered stabilization of E-cadherin in cell–cell junctions is a general phenomenon.

To quantify the E-cadherin staining at cell–cell junctions of different DDR1 expression clones, we performed linescan image analysis. The result showed that the average width of E-cadherin

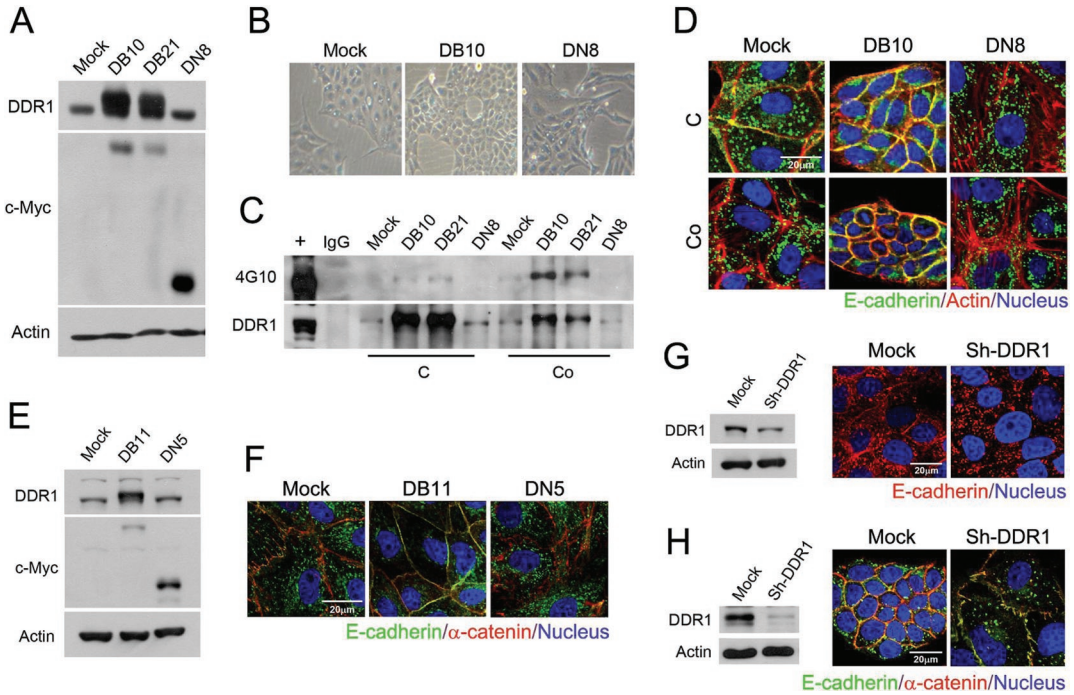

FIGURE 1: DDR1 promotes cell aggregation and localizes E-cadherin in cell–cell contacts. (A) LLC-PK1 cell harboring with control vector was used as control cells (mock). DB10 and DB21 were LLC-PK1 cells stably transfected with myc-tagged DDR1, and DN8 were cells expressed with myc-tagged dominant negative DDR1. Cells were incubated for 24 h, and levels of DDR1 were examined by immunoblotting using antibodies against either DDR1 or myc-tag. β-actin served as an internal control. (B) Phase-contrast images showed the cell morphology of mock, DB10, and DN8 after incubation for 24 h. (C) Phosphorylation levels of DDR1 in mock, DB10, DB21, and DN8 cells, cultured in a culture dish (C) or collagen-coated dish (Co) for 24 h, were assessed by immunoprecipitation of DDR1 and then immunoblotted with anti-phosphotyrosine antibody, 4G10, or anti-DDR1. (D) Mock, DB10, and DN8 cells were cultured in a culture dish (C) or collagen-coated dish (Co) for 48 h and then fixed and immunostained with anti-E-cadherin antibody followed by secondary antibody conjugative with Alexa-488 (green). F-actin was stained by phalloidin conjugated with TRITC (red). (E and F) Protein levels of DDR1 in different DDR1 expression clones of NMuMG cells were subjected to Western blot analysis (E) and immunofluorescence (F). For immunostaining, cells were incubated with E-cadherin and α-catenin antibodies followed by anti–mouse and anti–rabbit secondary antibody conjugated with Alexa-488 (green) and Alexa-594 (red). Both NMuMG and MDCK cells were used for knockdown experiments. (G) NMuMG cells expressed with scramble shRNA (mock) or shRNA for DDR1 (sh-DDR1) were subjected to immunoblotting and immunofluorescence. The localization of E-cadherin was examined and is shown in red. (H) The knockdown efficiency of DDR1 in MDCK cells was assessed by immunoblotting. The localization of E-cadherin and α-catenin was stained by specific antibodies followed by secondary antibodies conjugated with Alexa-488 (green) or Alexa-594 (red). Nuclei were stained by Hoechst 33258 (blue).

staining in the control LLC-PK1 cells is 1.27 ± 0.13 μm and that DB10 cells significantly increased it to 2.25 ± 0.12 μm (Supplemental Figure 1, A and C). In contrast, DN8 cells decreased the average width of E-cadherin in cell–cell junctions to 0.966 ± 0.09 μm (Supplemental Figure 1, A and C). In MDCK cells, DDR1 knockdown also significantly down-regulated E-cadherin width in cell–cell junctions compared with control cells (Supplemental Figure 1, B and D). These results indicate that DDR1 expression promotes junctional E-cadherin staining, whereas DN-DDR1 or knockdown of DDR1 decreases it.

DDR1 promotes cell differentiation and prevents collagen-induced dedifferentiation

To elucidate whether expression of DDR1 affected cell differentiation, a special structure known as microvilli in differentiated epithelial cells assessed by scanning electron microscopy (SEM). The results showed that microvilli were randomly spread on the cell surface and markedly decreased upon collagen stimulation in control cells, and were consistent with a previous report (Imamichi and Menke, 2007). DB10 cells had more microvilli when cultured without collagen, and collagen induced even higher numbers of microvilli. In contrast, the number of microvilli in DN8 cells was markedly reduced regardless of collagen treatment (Figure 2, A and B). Similar results were found in the different DDR1-expressing clones of MDCK cells (unpublished data). This result suggests that activation of DDR1 promotes cell differentiation and prevents collagen-induced dedifferentiation in epithelial cells.

To further determine the role of DDR1 in the regulation of epithelial cell characteristics, we assessed the EMT-related marker proteins, such as fibronectin, β1 integrin, E-cadherin, and α-SMA in both LLC-PK1 and NMuMG cells. DB10 cells displayed higher levels of E-cadherin but lower levels of fibronectin, β1 integrin, and α-SMA, whereas DN8 cells showed the opposite effects (Figure 2C, left). Knocking down DDR1 by shRNA in NMuMG cells displayed results similar to those of that by DN8 cells (Figure 2C, right). Immunofluorescence results further confirmed this finding. DB11 cells showed lower levels of fibronectin and α-SMA, whereas DN5 cells showed the opposite effects (Figure 2D). Strong staining of both fibronectin and α-SMA were also shown in sh-DDR1 cells (Figure 2E). We concluded that the expression of DDR1 promotes epithelial differentiation.

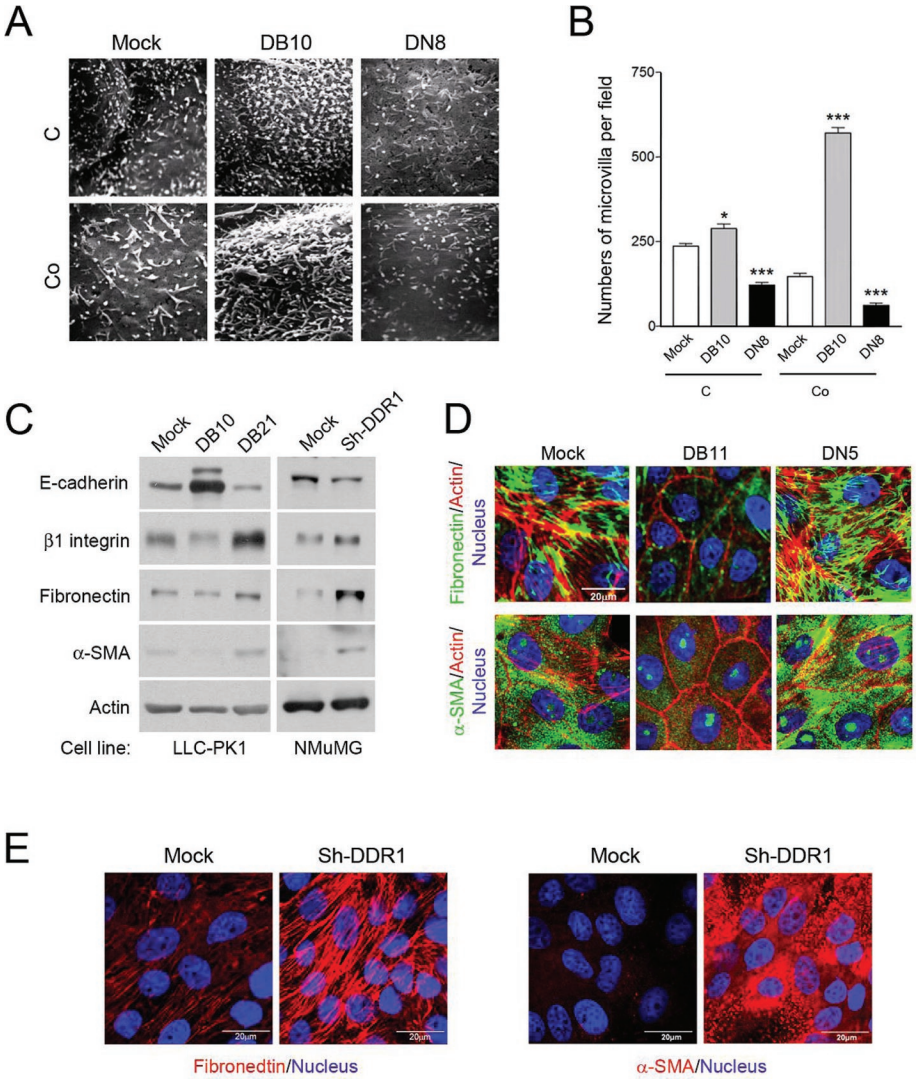

FIGURE 2: DDR1 promotes cell differentiation. (A) Various DDR1 expression clones of LLC-PK1 cells, including control (mock), DB10, and DN8, were incubated on coverslips with (Co) or without (C) collagen for 48 h. After cells were fixed, dehydrated, chemically dried, and coated with gold particles, the cell surface microvilli structure was examined by SEM. (B) The quantification results show the numbers of microvilli in each field from five different images. Each column represents the mean ± SE, and * or *** indicates $p < 0.05$ or $p < 0.001$, respectively. (C) Various DDR1 transfectants of LLC-PK1 and NMuMG were incubated for 24 h, and then the protein levels of fibronectin, β1 integrin, E-cadherin, and α-SMA were assessed by immunoblotting. (D) Expression of fibronectin and α-SMA in mock, DB11, or DN5 cells was examined by specific primary antibodies followed by secondary antibody conjugated with Alexa-488 (green). The organization of actin cytoskeleton was stained with phalloidin conjugated with TRITC (red). (E) Mock and sh-DDR1 clones of NMuMG cells were incubated for 24 h and then immunostained with antibody against fibronectin or α-SMA followed by secondary antibody conjugated with Alexa-594 (red). Nuclei were stained with Hoechst 33258 (blue).

To verify the expression and localization of DDR1 and E-cadherin, we transiently transfected myc-tagged DDR1 in LLC-PK1 cells and then cells were subjected for immunofluorescence study. The results showed that cells displaying higher DDR1 expression also showed higher E-cadherin staining, as indicated by white arrows (Supplemental Figure 2A). Enlarged figures further indicated that cells expressing higher levels of DDR1 showed strong E-cadherin staining in cell–cell junctions and a more compact phenotype compared with cells containing less exogenous DDR1. These results support our conclusion that expression of DDR1 increased E-cadherin levels. We further confirm the localization of endogenous DDR1 by using breast cancer cell lines, including MCF-7, MDA-MB-468, and MDA-MB-231. As shown in Supplemental Figure 2B, both MCF-7 and MDA-MB-468 expressed higher levels of E-cadherin and DDR1, but not MDA-MB-231, similar to previous reports (Dejmek *et al.*, 2005; Hansen *et al.*, 2006). The immunofluorescence study showed that the endogenous DDR1 was localized in cell–cell junctions and colocalized with E-cadherin in both MCF-7 and MDA-MB-468 cells (Supplemental Figure 2C). This result, together with our findings that DDR1 formed physical interaction with E-cadherin in different kinds of cell lines, such as MDCK, LLC-PK1, NMuMG, and A431 (Wang *et al.*, 2009), indicates that DDR1, regardless of endogenous or exogenous origin, is localized with E-cadherin in cell–cell junctions.

DDR1 promotes cell–cell adhesion but inhibits cell migration

To examine the functional role of DDR1 in epithelial differentiation, we performed the cell–cell adhesion and migration assays in different LLC-PK1 and MDCK clones. Compared with control cells, the DB10 cells significantly increased cell–cell adhesion ability within 24 h, whereas DN8 cells slightly decreased it. Collagen stimulation significantly suppressed cell–cell adhesion in both control and DN8 cells, but not DB10 cells (Supplemental Figure 3A). In MDCK cells, knockdown of DDR1 also significantly reduced cell–cell contacts regardless of collagen treatment (Supplemental Figure 3B). Expression of DDR1 decreased collagen-induced cell migration, whereas inhibition of DDR1 activation or knockdown of DDR1 increased it as described previously (Supplemental Figure 3, C–E) (Wang *et al.*, 2005). To examine the dynamic changes of cell–cell adhesion during cell migration, we observed changes of cell–cell adhesion and migration by the in vitro wound closure assay by using time lapse microscopy in live cells. The result showed that distance of sh-DDR1 cell migration was longer than that of control cells (Supplemental Figure 3, F and G) within 50 min. More importantly, after analysis of the dynamic morphological changes of ten cells in each clone at the intervals of 10 min, we found that the relative deformation ratio was increased in sh-DDR1 cells (Supplemental Figure 3H). These results indicate that expression of DDR1 promotes epithelial plasticity, including augmentation of cell–cell adhesion and reduced migratory ability.

DDR1 promotes the formation of E-cadherin–mediated junctional complexes

The results just mentioned revealed the regulation of cell–cell interaction and epithelial differentiation by DDR1. We sought to understand how DDR1 up-regulated E-cadherin expression. We found

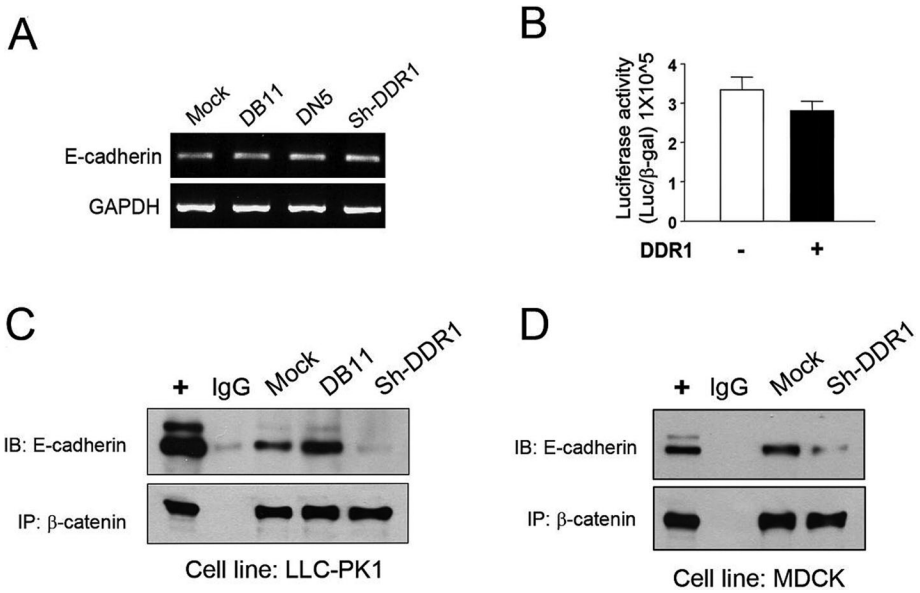

FIGURE 3: DDR1 increases the protein complexes of E-cadherin/β-catenin. (A) DDR1 expressing clones of NMuMG cells, including control (mock), DB11, DN5, and sh-DDR1 cells, were cultured in culture dishes for 24 h, and then the protein levels of E-cadherin were assessed by RT-PCR. (B) HEK293T cells transfected with DDR1 expression vector and/or E-cadherin–driven luciferase expression vector were subjected to promoter activity assay. Promoter activity was performed by normalization with β-gal activity in each condition. Each column represents the mean ± SE from three performances of independent experiments. (C) Different DDR1-expressing clones of NMuMG cells, including mock, DB11, and sh-DDR1 cells, were cultured in culture dishes for 24 h, and then the protein lysates were subjected to immunoprecipitation. E-cadherin/β-catenin complexes were assessed by adding anti–β-catenin antibody for immunoprecipitation, followed by immunoblotting with anti–E-cadherin antibody. (D) Protein complexes of E-cadherin/β-catenin were also assessed in sh-DDR1 of MDCK cells by immunoprecipitating with anti–E-cadherin antibody, followed by immunoblotting with anti–β-catenin antibody.

that mRNA and promoter activity of E-cadherin was not changed regardless of the levels of DDR1 (Figure 3, A and B), suggesting that transcriptional regulation was not involved in DDR1-increased E-cadherin protein levels. Because DDR1 regulated E-cadherin junctional localization, we investigated whether DDR1 increased E-cadherin protein abundance by maintaining the junctional complex of E-cadherin/β-catenin. Immunoprecipitation results showed that E-cadherin/β-catenin complexes were augmented in DB11 compared with control cells, whereas they were decreased in sh-DDR1 cells (Figure 3C). Similar results were obtained in sh-DDR1 MDCK cells, where E-cadherin/β-catenin complexes were decreased (Figure 3D). These results indicate that DDR1 promotes the formation of E-cadherin–mediated junctional complexes in epithelial cells.

DDR1 reduces degradation of E-cadherin

It has been shown that the stability of E-cadherin–mediated cell–cell contacts affects its recycling time and protein abundance (Su and Simmen, 2009), so we then investigated whether DDR1 reduces the degradation of E-cadherin. Various DDR1 expression clones of NMuMG cells were treated with cycloheximide (CHX) at different time points, and the levels of E-cadherin were assessed by Western blot analysis. After CHX treatment for 12 h, more than 89% of E-cadherin was preserved in DB11 cells, whereas only <40% of E-cadherin was observed in both DN5 and sh-DDR1 cells (Figure 4, A and B). Immunofluorescence results showed that E-cadherin formed disconnected staining in the cell–cell junction and many cytosolic spots in control cells (Figure 4C, indicated by open arrowhead). In DB11 cells, E-cadherin formed continuous staining along the cell–cell junction but not in the cytosol (Figure 4C). After CHX treatment for 8 h, E-cadherin largely disappeared from the cell–cell junction, indicated by arrows, in both control and DN5 cells, whereas E-cadherin still formed smooth bundles in the junctions in DB11 cells (Figure 4C). These results indicate that DDR1 stabilizes E-cadherin–mediated cell–cell junctions by decreasing degradation rate.

Endocytotic E-cadherin in early endosomes can be either delivered to lysosomes for degradation or recycled back to the cell membrane, depending on environmental cues (Bryant and Stow, 2004). To examine whether knockdown of DDR1 increases E-cadherin endocytosis, we observed localization of E-cadherin and early endosome marker EEA1 by dual immunostaining. In control cells, cytosolic E-cadherin was not colocalized with the early endosome. Knockdown of DDR1, however, augmented the colocalization of cytosolic E-cadherin and EEA1 (Figure 4, D and E). These results provide direct evidence of DDR1 in the reduction of the turnover rate of E-cadherin.

DDR1 decreases the dynamics of E-cadherin on cell membrane

To test whether DDR1 promotes E-cadherin–mediated cell–cell contact and then reduces the turnover of E-cadherin, we investigated the dynamic changes of E-cadherin on the cell membrane in different DDR1 expression clones. Live cell images were taken from cells expressing E-cadherin conjugated with mEos fluorescent protein (HECD-mEosFP). Fluorescence loss in photobleaching (FLIP) results showed that, with the same laser output, the regions with fluorescence loss was larger in sh-DDR1 cells (5 μm) than in mock cells (2.5 μm) (Figure 5A). The fluorescence loss then recovered in the photobleached sites in sh-DDR1 cells after 10 min, but this phenomenon was not significant in control cells (Figure 5A). The changes of fluorescence intensity in the photobleaching sites (region of interest [ROI] 4) or in adjacent areas (ROI5 and 6) were recorded and analyzed. ROI7 was used as the negative control in both control and sh-DDR1 cells. In control cells, loss of fluorescence intensity in ROI5 and 6 were approximately 26.06% and 45.79% (Figure 5B), whereas, in sh-DDR1 cells, it was enhanced to as high as 45.79% and 65.85% (Figure 5C). Statistical analysis showed that the average fluorescence intensity loss in control cells was approximately 26.81%, whereas sh-DDR1 cells significantly increased it to 50.39% (Figure 5D). The fluorescence intensity in ROI7 in both cells did not change during the recording time, suggesting that the fluorescence loss was due to photobleaching (Supplemental Figure 4). To further confirm that the fluorescence loss in ROI5 or 6 is due to the motility of E-cadherin, we fixed cells and observed cells under confocal microscopy. We found that one pulse of photobleaching markedly reduced the fluorescence intensity at ROI4. The fluorescence intensity in the regions around photobleaching sites (ROI5 and 6), however, was not changed (Supplemental Figure 5). These results support the conclusion that sh-DDR1 increases the membrane fluidity of E-cadherin. We then assessed the distance of fluorescence loss on the cell membrane after 1 s photobleaching. In control cells, the distance covering more than half of fluorescence intensity loss was ~4.56 μm

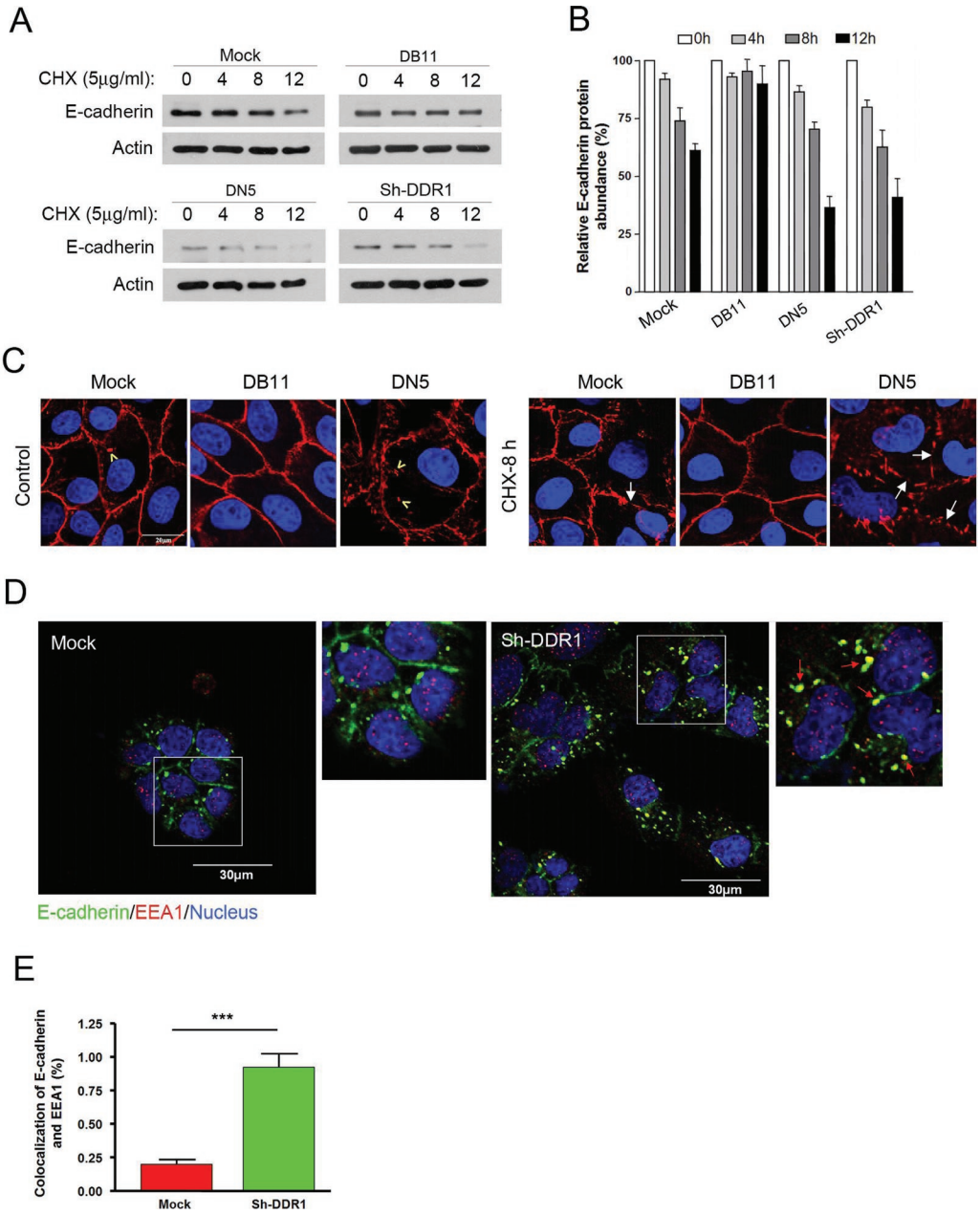

FIGURE 4: DDR1 reduces the turnover rate of E-cadherin by decreasing its endocytosis. (A) Different DDR1-expressing clones of NMuMG cells, cultured for 24 h, were treated with CHX at 5 μg/ml for the indicated time periods. The protein levels of E-cadherin were then assessed by immunoblotting. (B) Relative protein levels of E-cadherin in the DDR1 transfectants were quantified by normalization with actin. Each column represents the mean ± SE from three performances of independent experiments. (C) Localizations of E-cadherin in different clones before (0 h) or after CHX treatment for 8 h were immunostained with specific antibody followed by secondary antibody conjugated with Alexa-594 (red). The open arrowhead indicates the cytosolic E-cadherin staining, and the arrows indicate the loss of E-cadherin staining on the cell membrane. (D) Localization of E-cadherin (green) and EEA1 (red) were marked with specific antibodies in both control (mock) or sh-DDR1 clones of MDCK cells. The red arrow marks the colocalizations of E-cadherin and EEA1 in sh-DDR1 cells. (E) The percentage of E-cadherin with EEA1 colocalization was assessed by FV-1000 software, as estimated by the number of colocalized pixels / total number of positive pixels of E-cadherin. Each column represents the mean ± SE; ***$p < 0.001$.

on average (Figure 5E), whereas in sh-DDR1 cells this distance was markedly increased to 10.18 μm (Figure 5F). These results together show that DDR1 reduces the lateral diffusion rate of membrane-bound E-cadherin.

To understand whether E-cadherin can be recovered after long-term incubation, we then observed E-cadherin recovery by performing photoconversion in live cells. With photoconversion, the emission wavelength of mEos shifts from green to red. We found that red-HECD-mEosFP did not change its location within 60 min in control cells (Figure 6A and Supplemental Movie 1), whereas the red-HECD-mEosFP in the photoconversion site became dispersed, and some of the green-HECD-mEosFP moved into the regions with photoconversion within 30 min in shDDR1 cells (Figure 6B and Movie 2). The combination of photobleaching and photoconversion

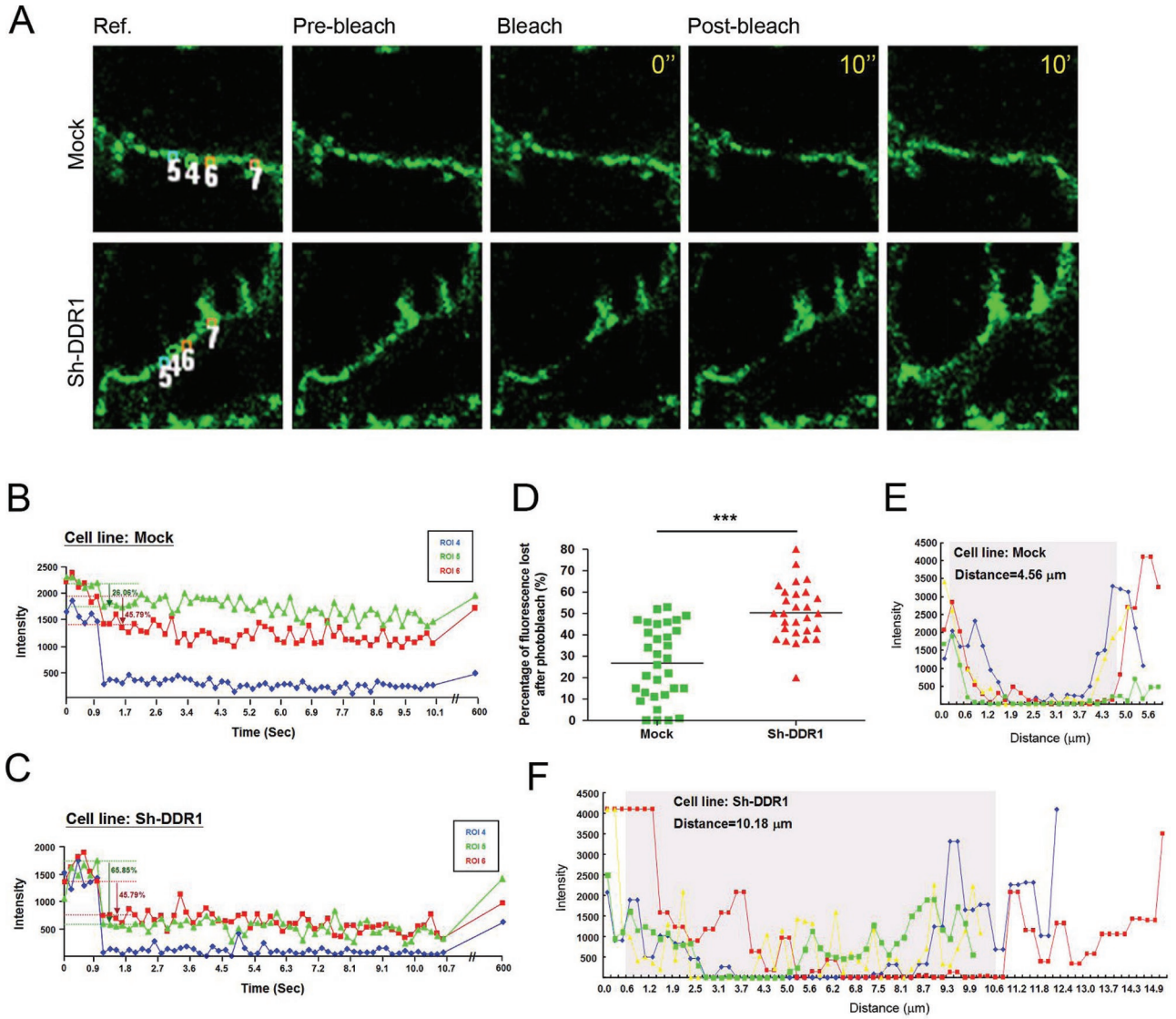

FIGURE 5: Determination of E-cadherin membrane stability by FLIP in different DDR1 expression clones. Control (mock) and sh-DDR1 MDCK cells were transiently transfected with HECD-mEosFP and cultured on coverslips for 48 h prior to the following experiments. (A) Fluorescence intensity of HECD-mEosFP in different clones was recorded before photobleaching for 1 s and followed by photobleaching for 100 ms at ROI4. Single section images were then collected at 0.17- to 0.18-s intervals for 9 s and at 10 min. The images before (prebleach), right after (bleach), or after (postbleach) photobleaching for the indicated times are shown (A). The line-graph shows the serial changes of fluorescence intensity within 10 min in mock (B) and sh-DDR1 (C) cells. ROI4, shown as a blue line, represents the changes of fluorescence intensity in the photobleaching site. ROI5 and 6, shown as green and red lines, were regions adjacent to the photobleaching site (ROI4). The diameter of each ROI is 1 μm, and the distance between ROI5 and ROI6 is within 5 μm. ROI7 was used as control for the fluorescence loss resulting from the 488-nm laser beam. (D) Percentage of fluorescence lost within ROI5 and 6 in mock (n = 32) and sh-DDR1 cells (n = 28) was assessed. ***$p < 0.001$. (E and F) A 1-s single bleach pulse of 1-μm diameter on the cell–cell junctions was performed in both mock (E) and sh-DDR1 (F) cells. Within 0.17 s after photobleaching, the fluorescence intensities at various distances from the photobleaching site were traced. Four representative experiments displaying the loss of fluorescence intensity in various distances after photobleaching are shown. The distance between the half-lost of the original fluorescence intensity on each side of photobleaching was assessed. The average distance of 50% loss of fluorescence intensity in mock and sh-DDR1 cells is shown in light purple shadow with 4.56 and 10.18 μm, respectively.

showed that red-HECD-mEosFP persisted around the photobleached site for at least 60 min in control cells (Figure 6C and Supplemental Figure 6A). Both the red-HECD-mEosFP and the photobleached site disappeared, however, within 30 min in sh-DDR1 cells (Figure 6D and Supplemental Figure 6B). The enlarged figures with pseudocolored red-HECD-mEos showed that the E-cadherin was more stable on the cell membrane in control than in sh-DDR1 cells (Figure 6C-vii and 6D-vii). In addition, we found that the red-HECD-mEosFP moved from the cell–cell junctions toward cytosol in sh-DDR1 cells (Figure 6D-vii). These studies further support the hypothesis that DDR1 increases the stability of E-cadherin–mediated cell–cell adhesion.

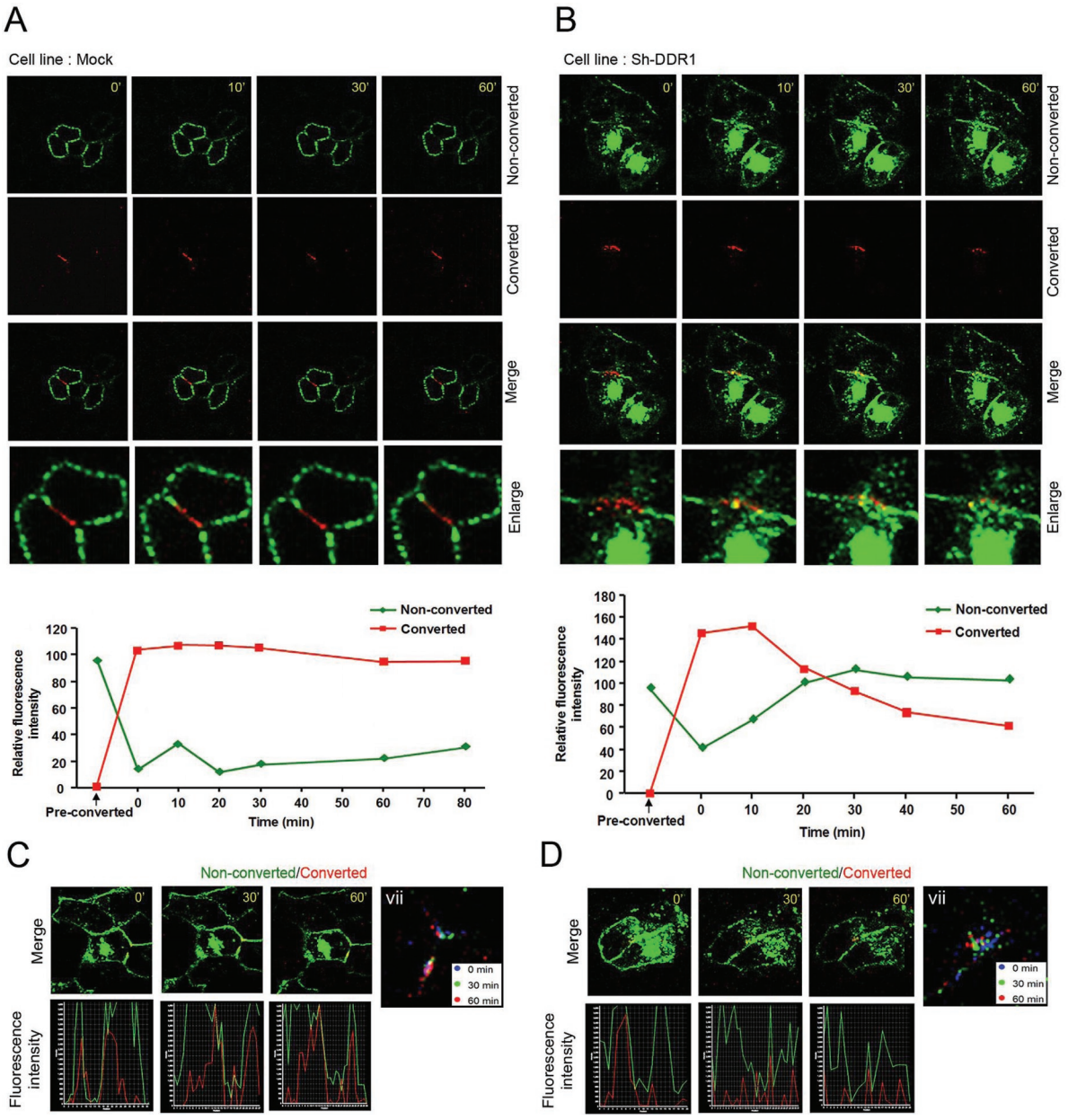

FIGURE 6: Determination of E-cadherin membrane stability by photoconversion in different DDR1 expression clones. The control (mock) and sh-DDR1 cells transiently transfected with HECD-mEosFP were incubated on coverslips for 48 h and then subjected to photoconversion analysis. The emission wavelength of 516 nm (green or nonconverted) or 581 nm (red or converted) of HECD-mEos before and after photoconversion by a 405-nm laser was recorded at the indicated times in mock (A) and sh-DDR1 (B) cells. Relative fluorescence intensity along the recording time is shown in the bottom panels. Photobleaching with higher laser output was applied after photoconversion in mock (C) and sh-DDR1 (D) cells. Photobleaching (100-ms) was used in a photoconverted area (red), and then the image of 516 and 581 nm was recorded for 60 min. The fluorescence intensity profiles on the cell membrane around the photoconversion site were assessed and are shown in the bottom panels. Images from the 581-nm laser at different time points (0, 30, and 60 min) were adjusted by software and are represented in pseudocolors, blue, green, and red (Cvii and Dvii).

Cdc42 activation mediates DDR1-regulated E-cadherin distribution

Our previous study showed that DDR1 suppresses Cdc42 and Rac1 activation (Yeh *et al.*, 2009), and one of their well-known functions is in maintaining E-cadherin–mediated cell–cell contacts (Bryant and Stow, 2004; Leibfried *et al.*, 2008; Hage *et al.*, 2009). To verify whether Cdc42 or Rac1 activation is involved in E-cadherin–mediated cell–cell adhesion induced by DDR1, we performed pull-down assays to examine the activity of either Cdc42 or Rac1. The results showed that knockdown of DDR1 significantly increased the activation of both Cdc42 and Rac1 compared with control cells (Figure 7, A and B). The localization of E-cadherin, however, did not change in both control and sh-DDR1 cells expressing either constitutively active (Rac1-L) or dominant negative (Rac1-N) Rac1 (Supplemental Figure 7). Both control and sh-DDR1 cells expressing Cdc42-L displayed loss of E-cadherin staining in cell–cell junctions. In contrast,

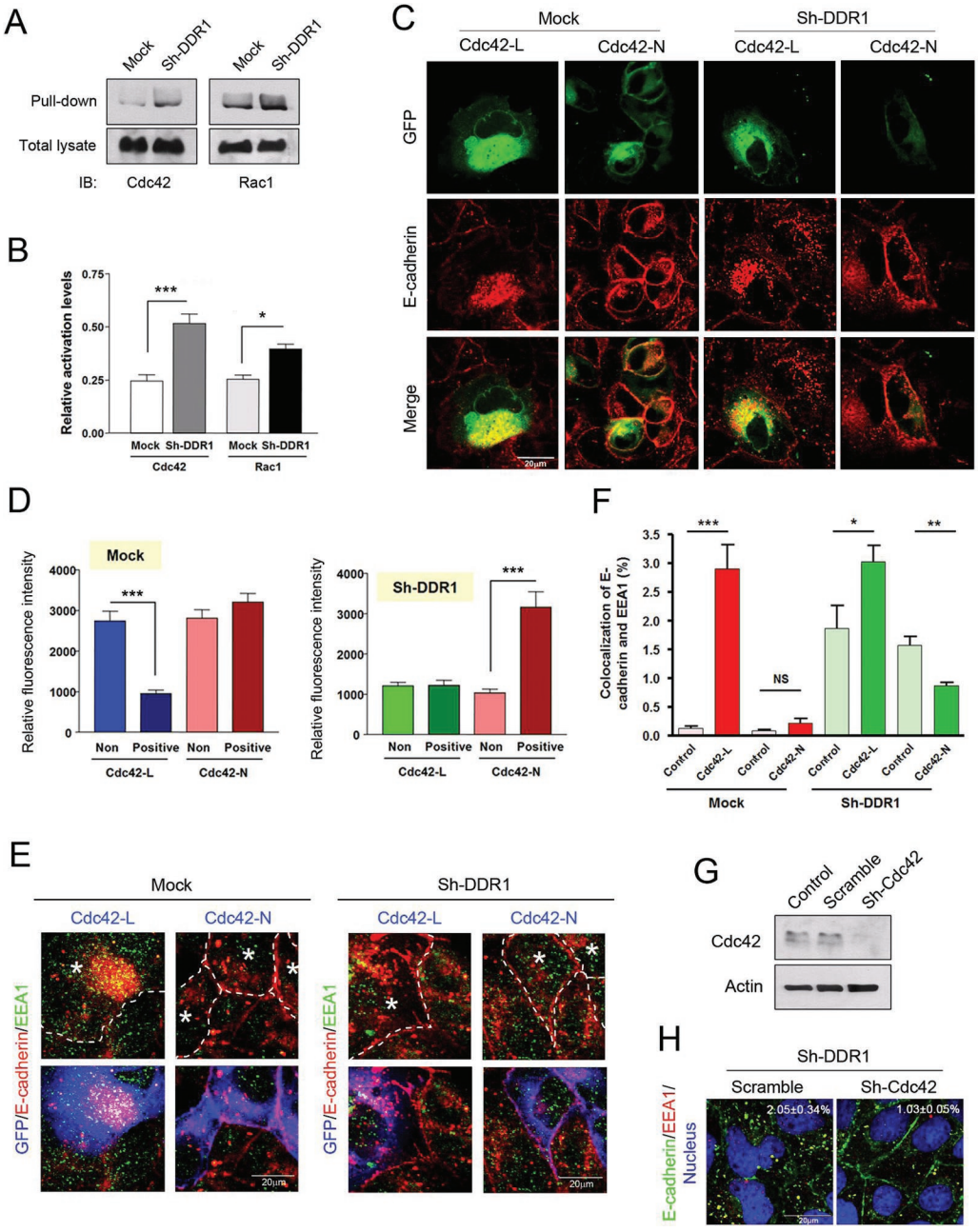

FIGURE 7: Deregulation of Cdc42 activity mediates DDR1-regulated E-cadherin membrane localization. (A) The control (mock) and sh-DDR1 MDCK cells cultured in culture dishes for 24 h were subjected to pull-down assay. (B) The relative activation levels of Cdc42 and Rac1 in mock and sh-DDR1 cells were quantified by normalization with their total protein level. Each bar represents the mean ± SE from three performances of independent experiments. * or *** indicates $p < 0.05$ or $p < 0.001$, respectively. Mock and sh-DDR1 cells transiently transfected with GFP-tagged (green) constitutive active (L) or dominant negative (N) Cdc42 were cultured in culture dishes for 24 h. (C) Localization of E-cadherin was labeled with specific antibody followed by secondary antibody conjugated with Alexa-594 (red). Nuclei were stained with Hoechst 33258 (blue). (D) The relative fluorescence intensity of E-cadherin on cell–cell junctions in cells expressed with or without Cdc42-L or Cdc42-N was assessed by FV-1000 software. More then 20 regions were selected from each of five pictures in every condition. Each bar represents the mean ± SE; ***$p < 0.001$. (E) Both mock and sh-DDR1 cells transiently transfected with GFP-tagged Cdc42-L or Cdc42-N were subjected to dual-staining of E-cadherin and EEA1. Stars indicate the positively transfected cell with a mutant form of Cdc42, as does blue color indicated in the bottom panel. The pseudocolors were used to represent the expression of the mutant form of Cdc42 (blue), E-cadherin (red), and EEA1 (green). (F) The percentage of E-cadherin with EEA1 colocalization was estimated by the normalized number of colocalized pixels with total number of positive pixels of E-cadherin. *, **, or *** indicates $p < 0.05$, $p < 0.01$, or $p < 0.001$, respectively. (G) Cdc42 expression in the control, scramble shRNA, and shRNA for Cdc42 (sh-Cdc42)-transfected cells was assessed by Western blot analysis. (H) The localization of E-cadherin (green) and EEA1 (red) in both scramble shRNA and sh-Cdc42 cells was examined by immunofluorescence. The colocalization percentages of E-cadherin and EEA1 in both scramble shRNA and sh-Cdc42 cells were assessed with FV-1000 software, and the results were 2.05 ± 0.186 and 1.03 ± 0.057, respectively.

expression of Cdc42-N induced cell aggregation and increased the membrane staining of E-cadherin (Figure 7C). The relative fluorescence intensity of E-cadherin in cell–cell junctions in cells expressing Cdc42-L or -N was then assessed. Control cells expressing Cdc42-L lost one-third of the E-cadherin fluorescence intensity on the cell membrane, whereas sh-DDR1 cells expressing Cdc42-N displayed a threefold increase of E-cadherin fluorescence intensity on the cell membrane (Figure 7D). These results indicate that DDR1 down-regulates Cdc42 activation then triggers the stabilization of membrane-bound E-cadherin.

To determine whether the activation of Cdc42 reduces membrane-bound E-cadherin by reorganizing actin cytoskeleton, dual-staining was used. Cdc42-L triggered cell spreading and actin stress fiber formation, and induced the accumulation of cytosolic E-cadherin staining in control cells. These characteristics were also found in sh-DDR1 cells. sh-DDR1 cells expressing Cdc42-N, however, displayed cortical actin and a less extensive phenotype (Supplementary Figure 8). These results suggest that Cdc42-induced actin reorganization reduced membrane stability of E-cadherin.

To test whether the activation of Cdc42 inhibits DDR1-induced E-cadherin stability, we then assessed the percentage of colocalization of E-cadherin and EEA1 in control and sh-DDR1 cells. Control cells expressed with Cdc42-L induced cytosolic E-cadherin staining and increased its colocalization with EEA1. In contrast, Cdc42-N expressing sh-DDR1 cells reduced the cytosolic E-cadherin and also the colocalization of E-cadherin with EEA1 (Figure 7, E and F). Moreover, we examined the effect of knockdown Cdc42 on localization of E-cadherin by using specific shRNA for Cdc42. Western blot analysis showed that sh-Cdc42 reduced 67% of endogenous Cdc42 protein levels but not the scramble shRNA (Figure 7G). Immunofluorescence results further showed that knockdown of Cdc42 reduced the cytosolic staining of E-cadherin and its colocalization with EEA1 from 2.05% to 1.03% (Figure 7H). Therefore we conclude that the activation of Cdc42 is responsible for DDR1-induced E-cadherin membrane stability.

DISCUSSION

In this study, we first provide evidence showing that DDR1 maintains E-cadherin–mediated cell–cell adhesion by inactivation of Cdc42 and thereby promotes differentiation in epithelial cells. Expression of DDR1 promoted the formation of E-cadherin/catenin complexes and cortical actin organization, which are the key elements in maintaining homo-E-cadherin stability. Images of live cells expressing E-cadherin conjugated with mEos fluorescent protein allowed us to monitor the mobility of E-cadherin in different DDR1 expression clones. Expression of DDR1 reduced the motility of E-cadherin on the cell membrane and then enhanced the half-life of E-cadherin; however, knockdown of DDR1 resulted in a higher diffusion rate of E-cadherin on the membrane and a shorter half-life. DDR1 suppressed the activation of Cdc42 and Rac1, but only the expression of Cdc42 mutant clones rescued the loss of E-cadherin in cell–cell junctions in sh-DDR1 cells. Overexpression of E-cadherin reduced β1 integrin gene expression by down-regulating its promoter activity. The β1 integrin signal is important in triggering EMT characteristics, such as up-regulation of α-SMA and fibronectin protein levels, and down-regulation of microvilli on the cell surface. DDR1 triggered cell differentiation through stabilization of E-cadherin–mediated cell–cell adhesion, which reduced β1 integrin gene expression and EMT. These results suggest opposing effects of DDR1 and β1 integrin in cell differentiation and imply that the signaling balance between DDR1 and β1 integrin is important in determining cell fate during differentiation (Figure 8).

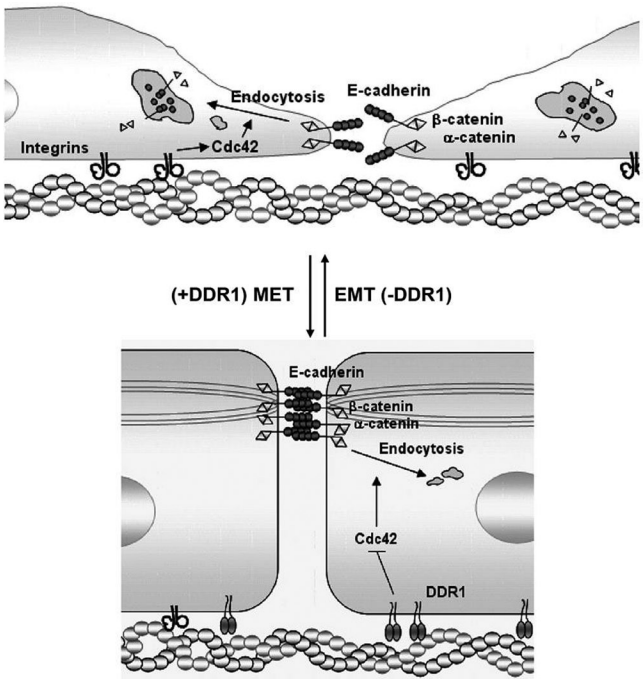

FIGURE 8: DDR1 promotes cell differentiation by stabilization of E-cadherin–mediated cell–cell adhesion. A proposed model illustrates the role of DDR1 in promoting epithelial cell differentiation through inhibiting the activation of Cdc42 and then maintaining E-cadherin–mediated cell–cell contacts.

Reciprocal regulation between E-cadherin and RTKs has been demonstrated in epidermal growth factor receptor, insulin-like growth factor receptor, and c-Met (Hoschuetzky *et al.*, 1994; Kimura *et al.*, 2006). This type of regulation has also been reported between E-cadherin and integrins (Kim *et al.*, 2009). Our recent work indicated a direct physical interaction between DDR1 and E-cadherin which in turn suppresses the activation of DDR1 and DDR1-inhibited cell spreading (Wang *et al.*, 2009). In this study, we discover that the activation of DDR1 promotes E-cadherin–mediated cell–cell adhesion through inactivation of Cdc42. These results indicate that DDR1 positively regulates E-cadherin–mediated cell–cell junction. E-cadherin, however, negatively controls the activation of DDR1. We propose that, when cells encounter junctional instability, for example, an increase in hepatocyte growth factor (HGF) or transforming growth factor-β1 (TGF-β1) signal, DDR1 is released from junctional complexes and is activated by collagen. The activation of DDR1 inhibits the β1 integrin signal which normally activates Cdc42. Because Cdc42 normally destabilizes E-cadherin/catenin complexes, its inhibition results in increased stability of the complexes. Therefore DDR1 activation results in increased junctional stability. After maturation of the adherent junction, DDR1 is recruited and its binding affinity to collagen is reduced. Our previous work also supports this hypothesis that knockdown E-cadherin expression induced loss of DDR1 staining from junctional sites but increase in basal sites (Wang *et al.*, 2009). The pathophysiological functions of DDR1, however (i.e., whether the DDR1 expression reduces TGF-β1–induced EMT or the TGF-β1 signal suppresses DDR1 expression during fibrosis), remain to be elucidated.

E-cadherin–mediated adhesion is critical in maintaining tissue architecture during development and tissue repair. This adhesion is tightly regulated, and the major pathway is through a gene regulatory mechanism (Huber *et al.*, 2005). Dynamic changes of

E-cadherin levels on cell membrane, however, are directly and effectively controlled by adherent junctional stability. Dynamic changes of E-cadherin levels occur in development, and several reports have shown that the dynamic of E-cadherin is required during cell migration (Fujita *et al.*, 2002; Palacios *et al.*, 2002). The membrane pool of E-cadherin is regulated by the balance between exocytosis and endocytosis, and the endocytic pathway is dominant in regulating this pool (Bryant and Stow, 2004). The endocytic E-cadherin is then either recycled to the cell membrane or degraded by lysosomes, depending on the environmental cues. Our studies showed that expression of DDR1 maintains the membrane stability of E-cadherin by reducing its endocytosis. In addition, DDR1 knockdown cells overexpressing E-cadherin (HECD-mEos) did not rescue the membrane stability, suggesting that the E-cadherin protein level was not sufficient to maintain junctional stability in our model system.

The functions of Rho family GTPases in maintaining the stability of adherent junctions is controversial. It has been shown that Rho family GTPases are involved in numerous cellular functions that are mediated mainly by controlling reorganization of the actin cytoskeleton (Hall, 1998). Activation of E-cadherin–mediated adherent junctions induces activation of Cdc42, Rac1, and RhoA, which further stabilize the junctions by reorganizing the actin cytoskeleton (Fukata and Kaibuchi, 2001). Activation of either type of small GTPase through different signaling pathways results in disruption of adherent junctions. Activation of Rac1 not only increases endocytosis of E-cadherin but also is responsible for collagen-induced down-regulation of E-cadherin (Shintani *et al.*, 2006). Cdc42 knockout induces abnormal accumulation of E-cadherin on the apical surface by reducing the endocytosis of E-cadherin (Georgiou *et al.*, 2008). Leibfried *et al.* have demonstrated the mechanism whereby Cdc42-Par6-a protein kinase C regulates the endocytosis of E-cadherin (Leibfried *et al.*, 2008). The actin bundles underneath the adherent junction are key elements in maintaining junctional stability, and α-catenin is the key regulator (Drees *et al.*, 2005). Activation of Cdc42 facilitates filamentous actin formation and promotes cell extension which may not support homophilic E-cadherin formation. In this study, we have shown that knockdown of DDR1 or expression of constitutively active Cdc42 promoted actin reorganization, cell extension, and, most of all, the internalization of E-cadherin. Recent studies have also demonstrated that the activation of Cdc42 mediated CHD1L-induced EMT in hepatocellular carcinoma cells (Chen *et al.*, 2010). These results suggest that Cdc42 activation is involved in DDR1-induced differentiation.

Early studies have reported that up-regulation of DDR1 occurs in fast-growing invasive tumors of the mammary gland, ovary, esophagus, growing brain, and lung (Johnson *et al.*, 1993; Laval *et al.*, 1994; Sanchez *et al.*, 1994; Alves *et al.*, 1995, 2001). A large-scale study of invasive ductal and lobular breast carcinoma samples has indicated that high expression of E-cadherin and DDR1 is restricted to ductal carcinomas (Turashvili *et al.*, 2007). In addition, Wnt-5a promotes DDR1 autophosphorylation and triggers epithelial phenotypic change in breast cancer cells (Jönsson and Andersson, 2001). This result suggests that DDR1 expression is prominent in differentiated tumors. The regulation and function, however, of DDR1 during cancer progression are still open questions. Recent studies demonstrate that different migratory patterns can be observed in cancer metastasis (Giampieri *et al.*, 2009; Tsuji *et al.*, 2009). Given that one of the functions of DDR1 is to stabilize cell–cell junctions, the DDR1-regulated E-cadherin in cell–cell junctions may be important for the regulation of collective cell migration, possibly in cancer metastasis.

MATERIALS AND METHODS

Cell culture and treatment

LLC-PK1, NMuMG, and MDCK cells were maintained as described previously (Yeh *et al.*, 2010). For experiments, cells were cultured at a density of 8×10^5 cells per 10-cm dish with or without collagen gel coating and then incubated with or without β1 integrin blocking antibody, HMβ1–1 (20 μg/ml; BioLegend, San Diego, CA) or HGF (5 ng/ml; Invitrogen, Carlsbad, CA).

Collagen was extracted from Wistar rat tail as described previously (Wang *et al.*, 2003). For preparation of 0.3% collagen gel, 3 ml of stock collagen solution was mixed with 1 ml of 5.7× DMEM, 0.5 ml of 2.5% $NaHCO_3$, 1 ml of 0.1 M HEPES, 0.1 ml of 0.17 M $CaCl_2$, 0.1 ml of 1 N NaOH, and 4.3 ml of culture medium.

Plasmid constructs

pcDNA3.1 expression vectors encoding myc-tagged DDR1, and myc-tagged carboxyl-terminal truncated (dominant-negative) DDR1 constructs were established previously (Wang *et al.*, 2005). For stable clone selection, LLC-PK1 and NMuMG cells were transfected with either myc-tagged DDR1 or DN-DDR1 and then treated with G418 sulfate at either 1 or 0.8 μg/ml for 2 wk (Table 1). The single colony was selected and resolved by SDS–PAGE.

pSM2 vector expressed shRNA against *Canis lupus familiaris* DDR1, and GPlz expression vector encoding shRNA against *Mus musculus* DDR1 was purchased from GenDiscovery Biotechnology (Taipei, Taiwan) (Table 1). The targeting sequences for *Canis lupus familiaris* and *Mus musculus* shRNA construct were: sense 5′- cgc agg tcc act gta aca aca t-3′ and antisense 5′- atg ttg tta cag tgg acc tgc a - 3′; the catalogue number is RHS1764–9217450 and sense 5′- cgc tgc tac tct tgg tga caa t -3′ and antisense 5′- att gtc acc aag agt agc agc a - 3′; the catalogue number is RMM4431–98695243, respectively. pLKO.1 vector expressed shRNA against *Canis lupus familiaris*. Cdc42 was also purchased from GeneDiscovery Biotechnology, and the target sequences were: sense 5′- cca aga aca aac aga agc cta - 3′ and antisense 5′- tag gct tct gtt tgt tct tgg - 3′ (catalogue number is RHS3979–9614830). Both DDR1 and Cdc42 knockdown stable clone were selected by adding puromycin at 0.5 to 1 μg/ml.

	Clones				
Cell line	Control vector	Overexpressing DDR1	Overexpressing DN-DDR1	Control vector	Knockdown DDR1
LLC-PK1	Mock (pcDNA3.1 vector)	DB10, DB21	DN8	–	–
NMuMG	Mock (pcDNA3.1 vector)	DB11	DN5	Mock (GPlz vector)	Sh-DDR1
MDCK	–	–	–	Mock (pSM2 vector)	Sh-DDR1

TABLE 1: Different DDR1 expression clones established in this study.

β1 integrin promoter (nucleotides –1057 to +77) was cloned from mouse kidney genomic DNA by using PCR amplification; the primer sequence for cloning is: 5′- tcc ctc ctc aag tca cac g -3′ and 5′- gct tct cgg ttg gtc tcg -3′. The promoter sequence was conjugated in pGL3-basic vector by using *Nhe*I and *Bgl*II restriction enzymes.

pcDNA3 expression vector-encoded human E-cadherin (HECD) was a gift from Barry M. Gumbiner (Memorial Sloan-Kettering Cancer Center, New York, NY). The p221-Ecadh-mEosFP was provided by Thomas Lecuit (Institut de Biologie du Developpment de Marseille Luminy, UMR 6216 CNRS-Universite de la Mediterranee, Marseille, France). We reconstructed these plasmids by amplifying the mEosFP by using PCR with the primers containing the *Xba*I cutting site: forward 5′- gct cta gag cgc cct cag aca cag act cc -3′ and reverse 5′- gct cta gag cat agt gac ctg ttc gtt gc-3′. Then the stop codon in HECD was changed to alanine by a site-directed mutagenesis kit with the primer sequences: forward, 5′-gcg gcg agg acg acg cgg ggt cta gag agc-3′ and reverse, 5′-gct ctc tag acc ccg cgt cgt cct cgc cgc-3′.

Immunoblot, immunoprecipitation, and pull-down assay

Cell lysates were harvested by RIPA buffer containing 50 mM Tris-HCl, pH 7.4; 150 mM NaCl; 1% Nonidet P-40; 0.5% sodium deoxycholate; 0.1% SDS; 1 mM sodium orthovanadate; and protease inhibitor cocktail. Protein lysate (20 μg) was resolved by SDS–PAGE followed by immunoblotting with antibodies against DDR1, α-catenin (Santa Cruz Biotechnology, Santa Cruz, CA), E-cadherin, β1 integrin, fibronectin (BD Biosciences PharMingen; San Jose, CA), α-SMA (Sigma-Aldrich, St. Louis, MO), and c-Myc (Oncogene Research Products, La Jolla, CA). For immunoprecipitation, 1 mg of protein lysate was incubated with 1 μg of primary antibody against DDR1 or β-catenin at 4°C overnight. After incubation with protein A-sepharose beads (Sigma Aldrich), the immunocomplex was then resolved by immunoblotting. Phosphorylation levels of DDR1 were detected by anti-phosphotyrosine antibody (clone 4G10; Millipore, Billerica, MA).

Cdc42 and Rac1 activation levels were assessed by using 1 mg of protein lysate incubated with 20 μg of GST-PAK-CD fused with glutathione sepharose beads followed by immunoblotting with anti-Cdc42 or Rac1 antibody, respectively. The GST-PAK-CD fusion with glutathione sepharose beads was prepared according to Yeh *et al.* (2009).

Reverse transcriptase-PCR

Reverse transcriptase-PCR (RT-PCR) was performed by using 0.2 μg of total RNA, extracted with an RNeasy Mini kit (Qiagen, Hilden, Germany) incubated with oligo-dT primer and Moloney murine leukemia virus RT (Promega, Madison, WI). The sequences of PCR primers were as follows: The *Mus musculus* β1 integrin (CD29) was designed from National Center for Biotechnology Information (NCBI) accession number NM_010578. The forward primer was 5′-ggt gtc gtg ttt gtg aat gc -3′, and reverse primer was 5′- ctc ctg tgc aca cgt gtc tt -3′. The resulting PCR product was 269 base pairs. PCR primer pair for *Mus musculus* E-cadherin (NCBI accession number NM_009864.2) was as follows: forward primer: 5′- cct gtc ttc aac cca agc ac-3′ and reverse primer: 5′-att tcc tga ccc aca cca aa-3′. The resulting PCR product was 398 base pairs.

Immunofluorescence, FLIP, and photoconversion

Cells were incubated at the indicated time and then fixed by 4% paraformaldehyde and permeabilized with 0.5% Triton X-100. Samples were incubated with specific primary antibody at 4°C overnight followed by incubating with Alexa-488 or -594–conjugated anti–mouse or –rabbit immunoglobulin G. Organization of actin cytoskeleton was examined by phalloidin-TRITC (Fluka, Buchs, Switzerland) and nuclei were stained by Hoechst 33258 (Molecular Probes, Carlsbad, CA). The immunofluorescence images were taken by confocal microscope (FV-1000; Olympus, Tokyo, Japan). FLIP was performed in MDCK clones transfected with E-cadherin–mEosFP. Cells cultured on coverslides for 48 h were subjected to the experiment. One single pulse of 405-nm laser beans with 10% laser output was used for photobleaching in a spot of 1 μm in diameter for 100 ms or 1 s. Fluorescence intensity in the photobleached site or beside it was traced in intervals of 0.17 to 0.18 s for 14 to 16 s. For photoconversion assays, 405-nm laser beans with 2% laser output were used. The changes in fluorescence intensity were recorded at indicated time points with FV-1000 software.

The image translation by cell migration or microscope stage movement at different time points was corrected back to the initial image by MATLAB software (MathWorks, Natick, MA). The cross-correlation function was used to identify the shift pixels in the images of nonconverted protein as compared to the initial frame. The image of converted protein in that frame was corrected by shifting the whole image back to the initial position. For illustrating the mobility of converted protein, the corrected images were then superimposed with blue, green, and red to demonstrate the protein distribution at 0, 30, and 60 min, respectively. High colocalization of merged color indicated less mobility of converted protein.

For E-cadherin and EEA1 colocalization analysis, two RGB fluorescence channels with individual thresholds of a minimum of 128 pixel intensity units (50%) were used. A colocalization algorithm in FV-1000 software was applied to assess the position and number of aligned positive (yellow) pixels, where colocalization (%) = number of colocalized pixels (between two channels of E-cadherin and EEA1) / total number of positive pixels of E-cadherin.

SEM

Cells were fixed with 4% glutaraldehyde and dehydrated by 100% ethanol. The specimens were subsequently processed with chemical drying, which in turn were soaked in 2 parts 100% ethyl alcohol/1 part hexamethyldisilazane (HMDS; Electron Microscopy Sciences, Fort Washington, PA) for 15 min, followed by 1 part 100% ethyl alcohol/2 parts HDMS for 15 min, and then two changes for 15 min each with 100% HDMS. Before mounting and sputter coating, the remaining HDMS was removed as cleanly as possible and allowed to dry in the chemical hood overnight.

Promoter activity assay

HEK293T cells were cotransfected with the reporter plasmids driven by β1 integrin, E-cadherin promoter, and/or expression vectors of pcDNA3.1-DDR1 or pcDNA3-HEDC. β-gal expression vector (a gift from Shaw-Jenq Tsai, National Cheng Kung University, Tainan, Taiwan) served as transfection control. A luciferase assay was performed by using Luciferase Assay Kit (Promega) according to the manufacture's protocol. Relative luciferase activity (arbitrary units) was reported after normalizing with β-gal activity (Su *et al.*, 2009).

Statistical analyses

All results were expressed as mean ± standard error of the mean and were analyzed by using Student's *t* test or one-way analysis of variance (ANOVA) using GraphPad Prism version 3.0 (GraphPad Software, San Diego, CA). Tukey's procedure was used to test the differences between individual treatment groups. Differences in comparison were considered as statistically significant when $p < 0.05$.

ACKNOWLEDGMENTS

We acknowledge financial support from the National Science Council (NSC 98–2627-B-006–007) and the National Health Research Institute (NHRI-EX-99–9840SI). We thank Ian Bruce for his helpful discussion and review of the manuscript. We gratefully acknowledge the provision of p-GL3 basic plasmid from Shaw-Jenq Tsai and technical assistance from Shih-Chieh Lin. We thank Tsi-Ling Chen for her administrative help.

REFERENCES

Adams CL, Chen YT, Smith SJ, Nelson WJ (1998). Mechanisms of epithelial cell-cell adhesion and cell compaction revealed by high-resolution tracking of E-cadherin-green fluorescent protein. J Cell Biol 142, 1105–1119.

Alves F, Saupe S, Ledwon M, Schaub F, Hiddemann W, Vogel WF (2001). Identification of two novel, kinase-deficient variants of discoidin domain receptor 1: differential expression in human colon cancer cell lines. FASEB J 15, 1321–1323.

Alves F, Vogel W, Mossie K, Millauer B, Hofler H, Ullrich A (1995). Distinct structural characteristics of discoidin I subfamily receptor tyrosine kinases and complementary expression in human cancer. Oncogene 10, 609–618.

Andl CD, Rustgi AK (2005). No one-way street: cross-talk between E-cadherin and receptor tyrosine kinase (RTK) signaling: a mechanism to regulate RTK activity. Cancer Biol Ther 4, 28–31.

Bryant DM, Stow JL (2004). The ins and outs of E-cadherin trafficking. Trends Cell Biol 14, 427–434.

Cavey M, Rauzi M, Lenne PF, Lecuit T (2008). A two-tiered mechanism for stabilization and immobilization of E-cadherin. Nature 453, 751–756.

Chen L *et al.* (2010). CHD1L promotes hepatocellular carcinoma progression and metastasis in mice and is associated with these processes in human patients. J Clin Invest 120, 1178–1191.

Cowin P, Rowlands TM, Hatsell SJ (2005). Cadherins and catenins in breast cancer. Curr Opin Cell Biol 17, 499–508.

Dejmek J, Leandersson K, Manjer J, Bjartell A, Emdin SO, Vogel WF, Landberg G, Andersson T (2005). Expression and signaling activity of Wnt-5a/discoidin domain receptor-1 and Syk plays distinct but decisive roles in breast cancer patient survival. Clin Cancer Res 11, 520–528.

Drees F, Pokutta S, Yamada S, Nelson WJ, Weis WI (2005). α-Catenin is a molecular switch that binds E-cadherin-β-catenin and regulates actin-filament assembly. Cell 123, 903–915.

Faraci E, Eck M, Gerstmayer B, Bosio A, Vogel WF (2003). An extracellular matrix-specific microarray allowed the identification of target genes downstream of discoidin domain receptors. Matrix Biol 22, 373–381.

Fujita Y, Krause G, Scheffner M, Zechner D, Leddy HE, Behrens J, Sommer T, Birchmeier W (2002). Hakai, a c-Cbl-like protein, ubiquitinates and induces endocytosis of the E-cadherin complex. Nat Cell Biol 4, 222–231.

Fukata M, Kaibuchi K (2001). Rho-family GTPases in cadherin-mediated cell-cell adhesion. Nat Rev Mol Cell Biol 2, 887–897.

Georgiou M, Marinari E, Burden J, Baum B (2008). Cdc42, Par6, and aPKC regulate Arp2/3-mediated endocytosis to control local adherens junction stability. Curr Biol 18, 1631–1638.

Giampieri S, Manning C, Hooper S, Jones L, Hill CS, Sahai E (2009). Localized and reversible TGFβ signaling switches breast cancer cells from cohesive to single cell motility. Nat Cell Biol 11, 1287–1296.

Gross O *et al.* (2004). DDR1-deficient mice show localized subepithelial GBM thickening with focal loss of slit diaphragms and proteinuria. Kidney Int 66, 102–111.

Hage B, Meinel K, Baum I, Giehl K, Menke A (2009). Rac1 activation inhibits E-cadherin-mediated adherens junctions via binding to IQGAP1 in pancreatic carcinoma cells. Cell Commun Signal 7, 23–35.

Hall A (1998). Rho GTPases and the actin cytoskeleton. Science 279, 509–514.

Hansen C, Greengard P, Nairn AC, Andersson T, Vogel WF (2006). Phosphorylation of DARPP-32 regulates breast cancer cell migration downstream of the receptor tyrosine kinase DDR1. Exp Cell Res 312, 4011–4018.

Hoschuetzky H, Aberle H, Kemler R (1994). Beta-catenin mediates the interaction of the cadherin-catenin complex with epidermal growth factor receptor. J Cell Biol 127, 1375–1380.

Huber MA, Kraut N, Beug H (2005). Molecular requirement for epithelial-mesenchymal transition during tumor progression. Curr Opin Cell Biol 17, 548–558.

Imamichi Y, Menke A (2007). Signaling pathways involved in collagen-induced disruption of the E-cadherin complex during epithelial-mesenchymal transition. Cells Tissues Organs 185, 180–190.

Johnson JD, Edman JC, Rutter WJ (1993). A receptor tyrosine kinase found in breast carcinoma cells has an extracellular discoidin I-like domain. Proc Natl Acad Sci USA 90, 5677–5681.

Jönsson M, Andersson T (2001). Repression of Wnt-5a impairs DDR1 phosphorylation and modifies adhesion and migration of mammary cells. J Cell Sci 114, 2043–2053.

Kalluri R, Neilson EG (2003). Epithelial-mesenchymal transition and its implications for fibrosis. J Clin Invest 112, 1776–1784.

Kim Y, Kugler MC, Wei Y, Kim KK, Li X, Brumwell AN, Chapman HA (2009). Integrin α3β1-dependent β-catenin phosphorylation links epithelial Smad signaling to cell contacts. J Cell Biol 184, 309–322.

Kimura T, Sakisaka T, Baba T, Yamada T, Takai Y (2006). Involvement of the Rac-Ras-activated Rab5 guanine nucleotide exchange factor RIN2-Rab5 pathway in the hepatocyte growth factor-induced endocytosis of E-cadherin. J Biol Chem 281, 10598–10609.

Knust E, Bossinger O (2002). Composition and formation of intercellular junctions in epithelial cells. Science 298, 1955–1959.

Lai C, Lemke G (1991). An extended family or protein-tyrosine kinase genes differentially expressed in the vertebrate nervous system. Neuron 6, 691–704.

Larue L, Ohsugi M, Hirchenhain J, Kemler R (1994). E-cadherin null mutant embryos fail to form a trophectoderm epithelium. Proc Natl Acad Sci USA 91, 8263–8267.

Laval S, Butler R, Shelling AN, Hanby AM, Poulsom R, Ganesan TS (1994). Isolation and characterization of an epithelial-specific receptor tyrosine kinase from an ovarian cancer cell line. Cell Growth Differ 11, 1173–1183.

Leckband D, Prakasam A (2006). Mechanism and dynamics of cadherin adhesion. Annu Rev Biomed Eng 8, 259–287.

Lee R, Eidman KE, Kren SM, Hostetter TH, Segal Y (2004). Localization of discoidin domain receptors in rat kidney. Nephron Exp Nephrol 97, e62–e70.

Leibfried A, Fricke R, Morgan MJ, Bogdan S, Bellaiche Y (2008). Drosophila Cip4 and WASp define a branch of the Cdc42-Par6-aPKC pathway regulating E-cadherin endocytosis. Curr Biol 18, 1639–1648.

Nelson WJ (2003). Adaptation of core mechanisms to generate cell polarity. Nature 422, 766–774.

Ohsugi M, Larue L, Schwarz H, Kemler R (1997). Cell-junctional and cytoskeletal organization in mouse blastocysts lacking E-cadherin. Dev Biol 185, 261–271.

Palacios F, Schweitzer JK, Boshans RL, D'Souza-Schorey C (2002). Arf6-GTP recruits NM23-H1 to facilitate dynamin-mediated endocytosis during adherens junctions disassembly. Nat Cell Biol 4, 929–936.

Perez JL, Jing SQ, Wong TM (1996). Identification of two isoforms of the Cak receptor kinase that are coexpressed in breast tumor cell lines. Oncogene 12, 1469–1477.

Pokutta S, Weis WI (2007). Structure and mechanism of cadherins and catenins in cell-cell contacts. Annu Rev Cell Dev Biol 23, 237–261.

Qian X, Karpova T, Sheppard AM, McNally J, Lowy DR (2004). E-cadherin-mediated adhesion inhibits ligand-dependent activation of diverse receptor tyrosine kinases. EMBO J 23, 1739–1748.

Sanchez MP, Tapley P, Saini SS, He B, Pulido D, Barbacid M (1994). Multiple tyrosine protein kinases in rat hippocampal neurons: isolation of Ptk-3, a receptor expressed in proliferative zones of the developing brain. Proc Natl Acad Sci USA 91, 1819–1823.

Shelling AN, Butler R, Jones T, Laval S, Boyle JM, Ganesan TS (1995). Localization of an epithelial-specific receptor (EDDR1) to chromosome 6p16. Genomics 25, 584–587.

Shintani Y, Wheelock MJ, Johnson KR (2006). Phosphoinositide-3 kinase-Rac1-c-Jun NH_2-terminal kinase signaling mediates collage I-induced cell scattering and up-regulation of N-cadherin expression in mouse mammary epithelial cells. Mol Biol Cell 17, 2963–2975.

Springer WR, Cooper DN, Barondes SH (1984). Discoidin I is implicated in cell-substratum attachment and ordered cell migration of Distyostelium discoideum and resembles fibronectin. Cell 39, 557–564.

Su HW, Wang SW, Ghishan FK, Kiela PR, Tang MJ (2009). Cell confluency-induced Stat3 activation regulates NHE3 expression by recruiting Sp1 and Sp3 to the proximal NHE3 promoter region during epithelial dome formation. Am J Physiol Cell Physiol 296, C13–C24.

Su Y, Simmen RC (2009). Soy isoflavone genistein up-regulates epithelial adhesion molecule E-cadherin expression and attenuates beta-catenin signaling in mammary epithelial cells. Carcinogenesis 30, 331–339.

Tsuji T, Ibaragi S, Hu GF (2009). Epithelial-mesenchymal transition and cell cooperativity in metastasis. Cancer Res 69, 7135–7139.
Tsukita SH, Tsukita SA, Nagafuchi A, Yonemura S (1992). Molecular linkage between cadherins and actin filaments in cell-cell adherens junctions. Curr Opin Cell Biol 4, 834–839.
Turashvili G *et al*. (2007). Novel markers for differentiation of lobular and ductal invasive breast carcinomas by laser microdissection and microarray analysis. BMC Cancer 7, 55–74.
Umbas R, Isaacs WB, Bringuier PP, Schaafsma HE, Karthaus HF, Oosterhof GO, Debruyne FM, Schalken JA (1994). Decreased E-cadherin expression is associated with poor prognosis in patients with prostate cancer. Cancer Res 54, 3929–3933.
Van Der Geer P, Hunter T, Lindberg RA (1994). Receptor tyrosine kinases and their signal transduction pathways. Annu Rev Cell Biol 10, 251–337.
Vleminckx K, Vakaet L. Jr., Mareel M, Fiers W, van Roy F (1991). Genetic manipulation of E-cadherin expression by epithelial tumor cells reveals an invasion suppressor role. Cell 66, 107–119.
Vogel W (1999). Discoidin somain receptors: structural relations and functional implications. FASEB J 13, 77–82.
Vogel W, Aszodi A, Alves F, Pawaon T (2001). Discoidin domain receptor 1 tyrosine kinase has an essential role in mammary gland development. Mol Cell Biol 21, 2906–2917.
Vogel W, Gish GD, Alves F, Pawaon T (1997). The discoidin domain receptor tyrosine kinases are activated by collagen. Mol Cell 1, 13–23.
Wang YK, Wang YH, Wang CZ, Sung JM, Chiu WT, Lin SH, Chang YH, Tang MJ (2003). Rigidity of collagen fibrils controls collagen gel-induced down-regulation of focal adhesion complex proteins mediated by $\alpha 2\beta 1$ integrin. J Biol Chem 278, 21886–21892.
Wang CZ, Hsu YM, Tang MJ (2005). Function of discoidin domain receptor I in HGF-induced branching tubulogenesis of MDCK cells in collagen gel. J Cell Physiol 203, 295–304.
Wang CZ, Su HW, Hsu YC, Shen MR, Tang MJ (2006). A discoidin domain receptor 1/SHP-2 signaling complex inhibits $\alpha 2\beta 1$-integrin-mediated signal transducers and activators of transcription 1/3 activation and cell migration. Mol Biol Cell 17, 2839–2852.
Wang CZ, Yeh YC, Tang MJ (2009). DDR1/E-cadherin complex regulates the activation of DDR1 and cell spreading. Am J Physiol Cell Physiol 297, 419–429.
Wheelock MJ, Shintani Y, Maeda M, Fukumoto Y, Johnson KR (2008). Cadherin switching. J Cell Sci 121, 727–735.
Wu H, Liang YL, Li Z, Jin J, Zhang W, Duan L, Zha X (2006). Positive expression of E-cadherin suppresses cell adhesion to fibronectin via reduction of $\alpha 5\beta 1$ integrin in human breast carcinoma cells. J Cancer Res Clin Oncol 132, 795–803.
Yeh YC, Wang CZ, Tang MJ (2009). Discoidin domain receptor 1 activation suppresses $\alpha 2\beta 1$ integrin-dependent cell spreading through inhibition of Cdc42 activity. J Cell Physiol 218, 146–156.
Yeh YC, Wei WC, Wang YK, Lin SC, Sung JM, Tang MJ (2010). TGF-$\beta 1$ induces Smad3-dependent $\beta 1$ integrin gene expression in epithelial-to-mesenchymal transition during chronic tubulointerstitial fibrosis. Am J Pathol 177, 1743–1754.
Zerlin M, Julius MA, Goldfarb M (1993). NEP: a novel receptor-like tyrosine kinase expressed in proliferating neuroepithelia. Oncogene 8, 2731–2739.
Zheng G *et al*. (2009). Disruption of E-cadherin by matrix metalloproteinase directly mediates epithelial-mesenchymal transition downstream of transforming growth factor-$\beta 1$ in renal tubular epithelial cells. Am J Pathol 175, 580–591.